Inorg. Chem. **2004**, *43*, 1976–1985

Ion Chemistry of $OV(OCH_3)_3$ in the Gas Phase: Molecular Cations and Anions and Their Primary Fragmentations

Detlef Schröder,*,† Jessica Loos,† Marianne Engeser,† Helmut Schwarz,† Hans-Christian Jankowiak,† Robert Berger,† Roland Thissen,‡ Odile Dutuit,‡ Jens Döbler,§ and Joachim Sauer§

Institut für Chemie der Technischen Universität Berlin, Strasse des 17 Juni 135, D-10623 Berlin, Germany, Laboratoire de Chimie Physique, Bat. 350, Université Paris-Sud, 91405 Orsay, France, and Institut für Chemie der Humboldt Universität Berlin, Unter den Linden 6, D-10099 Berlin, Germany

Received August 28, 2003

Trimethyl vanadate(V), $OV(OCH_3)_3$ (**1**), is examined by various mass spectrometric means. Photoionization experiments yield an ionization energy of $IE(OV(OCH_3)_3) = 9.54 \pm 0.05$ eV for the neutral molecule. The primary fragmentation of the molecular cation $\mathbf{1}^+$, i.e., loss of neutral formaldehyde, can occur via two independent routes of hydrogen migrations to afford the formal V^{IV} compounds $HOV(OCH_3)_2^+$ and $OV(OCH_3)(CH_3OH)^+$, respectively. These two pathways are associated with low-lying activation barriers of almost identical height. At elevated energies, direct V–O bond cleavage of $\mathbf{1}^+$ allows for expulsion of a methoxy radical concomitant with the generation of the cationic fragment $OV(OCH_3)_2^+$, a formal V^V compound. Trimethyl vanadate can also form a molecular anion, $\mathbf{1}^-$, whose most abundant dissociation channel involves loss of a methyl radical, thereby leading to the formal V^V compound $OV(OCH_3)_2O^-$. Various mass spectrometric experiments and extensive theoretical studies provide detailed insight into the ion structures and the relative energetics of the primary dissociation reactions of the molecular cations and anions of **1**.

1. Introduction

Transition-metal alkoxides are important in various areas of chemistry as they exhibit interesting properties as bulk materials. Our particular interest in metal alkoxides arises from their potential role in metal-mediated oxidation reactions. Activation of an alkane R−H by a reactive metal−oxo species [M]═O, present on a catalytically active surface, can occur via formal σ-bond metathesis for which two options exist (Scheme 1): either hydrogen adds to oxygen and the alkyl residue is bonded to the metal (route a), or C−O bond formation yields a metal alkoxide with an additional [M]−H bond (route b).

In the case of the activation of methane by the bare FeO^+ cation, a prototype reaction for the bond activation of an alkane by a transition-metal oxide in the gas phase,[1,2] ab initio studies of Yoshizawa and co-workers[3] predict a clear preference for route a. Nevertheless, also the intermediacy of metal alkoxides (route b) is not too energy demanding for the methane/FeO^+ system and therefore worth considering.[3] Formation of metal alkoxides has also been proposed in the reactions of other metal−oxo complexes with alkanes[4,5] and is of crucial importance in the dihydroxylation of olefins by high-valent metal oxides such as OsO_4.[6] Furthermore, intermediate metal alkoxides may hinder the release of alkanols (ROH), often the desired products in partial oxida-

Scheme 1

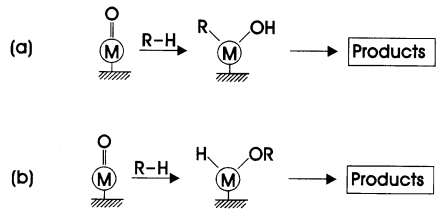

* Author to whom correspondence should be addressed.
† Institut für Chemie der Technischen Universität Berlin.
‡ Laboratoire de Chimie Physique.
§ Institut für Chemie der Humboldt Universität Berlin.

(1) Schröder, D.; Schwarz, H. *Angew. Chem.* **1995**, *107*, 2126; *Angew. Chem., Int. Ed. Engl.* **1995**, *34*, 1973.
(2) Schröder, D.; Shaik, S.; Schwarz, H. In *Metal-Oxo and Metal-Peroxo Species in Catalytic Oxidations*; Meunier, B., Ed.; *Structure and Bonding*, Vol. 97; Springer: Berlin, 2000; p 91.
(3) Yoshizawa, K.; Shiota, Y.; Yamabe, T. *Chem.—Eur. J.* **1997**, *3*, 1160.
(4) Deng, L.; Ziegler, T. *Organometallics* **1996**, *15*, 3011.
(5) Fiedler, A.; Kretzschmar, I.; Schröder, D.; Schwarz, H. *J. Am. Chem. Soc.* **1996**, *118*, 9941.
(6) Smith, M. B.; March, J. *March's Advanced Organic Chemistry*; Wiley: New York, 2001; p 1048 ff.

10.1021/ic030264x CCC: $27.50
Published on Web 02/18/2004

tion of RH, from the active metal centers present on the surface of a catalyst. This aspect is quite important in selective partial oxidation because the primary oxygenation product ROH is usually more easily oxidized than the alkane RH, e.g., $D_0(H-CH_2OH) = 4.10$ eV versus $D_0(H-CH_3) = 4.48$ eV.[7] In turn, this reaction is important when oxidation to carbonyl compounds is desired, e.g., the conversion of methanol into formaldehyde performed on copper contacts.

Our present investigation is part of collaborative experimental and theoretical efforts in the Berlin area[8] on the mechanisms of oxidation reactions catalyzed by transition-metal oxides. A particular focus lies on vanadium oxide catalysts which have widespread applications in redox reactions.[9] For example, $V-O-CH_3$ surface species are intermediates in the selective oxidation of methanol to formaldehyde.[10] Within this context, the gas-phase chemistry of ionized trimethyl vanadate(V), $OV(OCH_3)_3$ (**1**), shall provide a benchmark for various experimental and theoretical studies on vanadium oxides.

2. Methods

Exploratory experiments were performed with a modified VG ZAB/HF/AMD 604 four-sector mass spectrometer of BEBE configuration (B stands for magnetic and E for electric sector) which has been described elsewhere.[11] In brief, cations were generated by electron ionization (EI) of **1** introduced via a solid probe. After acceleration to a kinetic energy of 8 keV, the ions of interest were mass-selected and subjected to metastable ion (MI) and collisional activation (CA) studies. MI spectra of B(1)/E(1) mass-selected ions were recorded by detection of the charged fragments formed unimolecularly in the field-free region between E(1) and B(2) by scanning the latter sector. CA spectra were obtained in the same manner, except that helium (80% transmittance, T) was used as a stationary collision gas. In addition, the molecular anion $\mathbf{1}^-$ was generated using N_2O as a reagent gas and characterized by CA as well as charge reversal (CR),[12] neutralization−reionization (NR),[13,14] and the related NIDD method (NIDD = neutral and ion decomposition difference);[15] in CR and NR, oxygen (80% T) was used as a collision gas.

Photoionization (PI) studies were performed in the CERISES apparatus[16] installed on the beam line SA63 of the synchrotron radiation source SuperACO at LURE (Orsay, France). This beam line is a normal incidence monochromator which operates in the range of 7−30 eV photon energy. Slits were opened to 1 mm, corresponding to a photon-energy resolution of about 500 (i.e., 20 meV at 10 eV). The accuracy of the photon energy was verified by measuring the ionization energy of argon within 2 meV of its nominal value. At photon energies <11.8 eV, a LiF window was used to effectively eliminate higher-order light emerging from the grating of the monochromator. The experiments without a LiF filter were inherently interfered with higher-order photons and are reported without corrections. Neutral **1** is sufficiently volatile for introduction via a regular gas inlet. The neutral species were ionized by monochromatized photons, and the electrons and cations formed were extracted in opposite directions by a field of 1 V/cm. In the present experiments, electrons of low kinetic energies are detected without detailed velocity analysis, and the cations are transferred into a QOQ system (Q stands for quadrupole and O for octopole), Q2 of which was scanned for mass analysis. Cations were detected by a multichannel plate operating in the counting mode. Unfortunately, compound **1** leads to a serious contamination of the ion source of CERISES. Moreover, the electron detector mounted spatially close to the ionization volume showed a continuous decrease in performance when exposed to **1**. Given the strict time schedule at a synchrotron facility, also traces of 3-methyl[4-D_1]-valeramide examined the days before in another project were still present. For these reasons, the PI experiments were limited to the formation of the molecular ion $\mathbf{1}^+$ and its primary photofragments. Some experiments were also performed in the coincidence mode (TPEPICO = threshold-photoelectron photoion coincidence),[17] but due to the decreasing performance of the electron detector in the presence of **1**, only a few data points could be collected, which are insufficient for the construction of a breakdown graph. Appearance energies of the photofragments were determined by extrapolating the linear parts of the respective single-ion monitoring curves to the baseline. The error estimates given refer to these extrapolations; neither thermal contributions nor kinetic shifts were considered.

Compound **1** was prepared by reaction of $OVCl_3$ with sodium methoxide in dry diethyl ether and purified by recrystallization from pentane. Likewise, fully deuterated $OV(OCD_3)_3$, $\mathbf{1}_D$, was prepared from $OVCl_3$ and CD_3OLi and purified by sublimation (1 mbar, 80 °C). The synthesis and the transport of the samples require the use of inert gases, while the compounds are stable enough to tolerate short contact with the atmosphere during introduction into the mass spectrometer. For the photoionization studies, however, the sample was handled in a glovebox.

All calculations employed the density functional theory (DFT) modules of the Turbomole 5.5 suite,[18] specifically Becke's three-parameter hybrid functional B3-LYP[19,20] and Becke's exchange functional with Perdew's gradient-corrected correlation functional (B-P86)[21] as implemented in Turbomole. The B-P86 functional was used in conjunction with the resolution of the identity (RI) technique,[22,23] which approximates the computationally demanding four-center integrals by more simple three-center integrals using an auxiliary basis without a considerable degradation of the results. All structures were optimized in all-electron Kohn−Sham calculations employing Ahlrichs' valence triple-ζ basis sets with polarization functions on all atoms (TZVP).[24] The two different functionals

(7) Berkowitz, J.; Ellison, G. B.; Gutman, D. *J. Phys. Chem.* **1994**, *98*, 2744.
(8) Sonderforschungsbereich 546. Structure, dynamics and reactivity of transition-metal oxide aggregates. http://www.chemie.hu-berlin.de/sfb546/index.html.
(9) *Appl. Catal. A* **1997**, 157 (the entire volume deals with this topic).
(10) Weckhuysen, B. M.; Keller, D. E. *Catal. Today* **2003**, *78*, 25.
(11) Schalley, C. A.; Schröder, D.; Schwarz, H. *Int. J. Mass Spectrom. Ion Processes* **1996**, *153*, 173.
(12) Bursey, M. M. *Mass Spectrom. Rev.* **1990**, *9*, 555.
(13) Goldberg, N.; Schwarz, H. *Acc. Chem. Res.* **1994**, *27*, 347.
(14) Tureček, F. *Top. Curr. Chem.* **2003**, *225*, 77.
(15) Schalley, C. A.; Hornung, G.; Schröder, D.; Schwarz, H. *Chem. Soc. Rev.* **1998**, *27*, 91.
(16) Dutuit; O.; Alcaraz, C.; Gerlich, D.; Guyon, P. M.; Hepburn, J. W.; Metayer-Zeitoun, C.; Ozenne, J. B.; Weng, T. *Chem. Phys.* **1996**, *209*, 177.
(17) Baer, T. In *Gas-Phase Ion Chemistry*; Bowers, M. T., Ed.; Academic Press: New York, 1979; Vol. 1, p 153.
(18) Ahlrichs, R.; Bär, M.; Häser, M.; Horn, H.; Kölmel, C. *Chem. Phys. Lett.* **1989**, *162*, 165.
(19) Becke, A. D. *J. Chem. Phys.* **1993**, *98*, 5648.
(20) Stephens, P. J.; Derlin, F. J.; Chabalowski, C. F.; Frisch, M. J. *J. Phys. Chem.* **1994**, *98*, 11623.
(21) (a) Perdew, J. P. *Phys. Rev. B* **1986**, *33*, 8822. (b) Becke, A. D. *Phys. Rev. A* **1988**, *38*, 3098.
(22) Eichkorn, K.; Treutler, O.; Öhm, H.; Häser, M.; Ahlrichs, R. *Chem. Phys. Lett.* **1995**, *240*, 283.
(23) Eichkorn, K.; Weigend, F.; Treutler, O.; Ahlrichs, R. *Theor. Chem. Acc.* **1997**, 97, 119.
(24) Schäfer, A.; Huber, C.; Ahlrichs, R. *J. Chem. Phys.* **1994**, *100*, 5829.

used (B3-LYP and B-P86) agree well as far as relative energies are concerned. For the sake of brevity, only B3-LYP energies are reported here because this hybrid functional shows a somewhat better performance in the prediction of thermochemical data.[25] Harmonic vibrational frequencies were calculated from analytical second derivatives of the total electronic energy. The optimized structures are visualized with the program Molden.[26] The transition structures for hydrogen migrations within the cation $\mathbf{1}^+$ (see below) were located with Gaussian 98,[27] using B3-LYP in conjunction with the QST (quadratic synchronous transit) approach, followed by energy calculations as well as gradient and second-derivative calculations with Turbomole. Recalculation of the energy is necessary due to different implementation of some functionals in the two program packages. However, the gradients calculated with Turbomole were small so that the effect on the structures was considered negligible. Using the harmonic frequencies, thermodynamic properties at 0 and 298 K were computed with the program Viewmol 2.3.

On the basis of the B3-LYP results, the Franck−Condon factors, which determine the vibrational fine structure of the photoionization process, have been obtained along the lines of a procedure described previously.[28] Briefly, the equilibrium structures of the electronic ground states of the neutral species and of the molecular cation together with the corresponding unscaled harmonic force fields were used to obtain the multidimensional Franck−Condon integrals with the aid of the recurrence formulas derived by Doktorov, Malkin, and Man'ko,[29] which take mode mixing effects and geometrical changes into account.[30] Although the computational scheme described in ref 28 allows for separable one-dimensional anharmonic treatments, all internal degrees of freedom of the molecular systems studied here were considered as harmonic modes. Each of the equivalent C_1-symmetric structures of the cation was treated as an isolated minimum, and couplings between the vibrational levels of these structures were neglected. The Franck−Condon profiles have been calculated for 0 K; no major changes of the Franck−Condon envelope for ionization of **1** and $\mathbf{1}_D$ were found for a vibrational Boltzmann distribution at 298 K. The corresponding quantum number combinations of the numerous vibrational overlap integrals have been generated with an algorithm described elsewhere.[31] From the resulting Franck−Condon envelope, the relative energy-dependent photoionization cross-sections have been obtained assuming a stepwise increase of the photoionization cross-section for each vibronic transition.

3. Experimental Results

EI mass spectra of several trialkyl vanadates(V) have already been reported by Adler et al. in 1976.[32] Unlike the larger homologues, the trimethyl compound $OV(OCH_3)_3$, **1**, gives rise to an abundant molecular ion, $\mathbf{1}^+$ ($m/z = 160$), with an intensity of ca. 20% relative to the base peak at $m/z = 130$. The latter is part of a "quartet" of fragment ions between $m/z = 127$ and $m/z = 130$ with intensities of ca. 70:20:20:100 upon EI, a spectral feature to which we return further below. In addition, loss of atomic hydrogen, $[\mathbf{1} - H]^+$ ($m/z = 159$), was observed by Adler et al. along with some consecutive fragmentations. Our EI measurements are fully consistent with these earlier data. Investigation of the perdeuterated compound $OV(OCD_3)_3$ (**1**) further allows the quartet of fragments (shifted to $m/z = 131$, 133, 135, and 137) to be assigned to formal losses of CX_nO (X = H, D; $n = 5-2$), respectively, from the molecular ion. In the following sections, the dissociation behavior of the molecular ion $\mathbf{1}^+$ is examined by several mass spectrometric means. In addition, the fragmentations of the molecular anion $\mathbf{1}^-$ and of the potassium adduct $[\mathbf{1}\cdot K]^+$ are discussed briefly.

3.1. Fragmentation Behavior of $\mathbf{1}^+$. The MI spectrum of mass-selected $\mathbf{1}^+$ recorded in the sector-field mass spectrometer is dominated by expulsion of formaldehyde ($\Delta m = -30$) along with small amounts of H_2 and CH_4O losses (Table 1). The formal elimination of CH_4O ($\Delta m = -32$) may be assigned to either consecutive expulsions of CH_2O and H_2 or the generation of an intact methanol molecule. Upon CA, loss of atomic hydrogen to afford $[\mathbf{1} - H]^+$ appears as a new channel, and the fragments observed between $\Delta m = -30$ and $\Delta m = -33$ resemble the quartet observed in the EI mass spectrum. The notable signal for $\Delta m = -31$ evolving upon CA can clearly be assigned to the loss of an intact methoxy group from $\mathbf{1}^+$. Absence of this channel in the MI spectrum implies that direct V−O bond cleavage is a high-energy process which is inaccessible for metastable $\mathbf{1}^+$.

Similar to the molecular ion $\mathbf{1}^+$, the MI and CA spectra of $[\mathbf{1} - H]^+$ are characterized by losses of formaldehyde ($\Delta m = -30$). Upon CA, also expulsions of CH_3O and CH_4O are observed. In contrast, the MI spectra of the ions $[\mathbf{1} - CH_2O]^+$ and $[\mathbf{1} - CH_3O]^+$ both show pronounced dehydrogenations ($\Delta m = -2$) in that considerable percentages of the mass-selected ions decompose in the field-free region (see footnotes *b* and *c* of Table 1); usually, the fraction of decomposing ions is far below 1% in MI spectra.[33] Obviously, loss of molecular hydrogen is particularly facile for these two ions formed upon dissociative EI of **1**. Therefore, not surprisingly, also the corresponding CA spectra are dominated by dehydrogenation. The consecutive dehydrogenation reactions provide a rationale for the quartet observed between $m/z = 127$ and $m/z = 130$. Loss of formaldehyde from $\mathbf{1}^+$ ($m/z = 160$) gives rise to $m/z = 130$, which then

(25) Koch, W.; Holthausen, M. C. *A Chemist's Guide to Density Functional Theory*; Wiley-VCH: Weinheim, Germany, 2000; p 137.
(26) Schaftenaar, G.; Noordik, J. H. *J. Comput.-Aided Mol. Des.* **2000**, *14*, 123.
(27) Gaussian 98, Revision A.7: Frisch, M. J.; Trucks, G. W.; Schlegel, H. B.; Scuseria, G. E.; Robb, M. A.; Cheeseman, J. R.; Zakrzewski, V. G.; Montgomery, J. A., Jr.; Stratmann, R. E.; Burant, Dapprich, S.; Millam, J. M.; Daniels, A. D.; Kudin, K. N.; Strain, M. C.; Farkas, O.; Tomasi, J.; Barone, V.; Cossi, M.; Cammi, R.; Mennucci, B.; Pomelli, C.; Adamo, C.; Clifford, S.; Ochterski, J.; Petersson, G. A.; Ayala, P. Y.; Cui, Q.; Morokuma, K.; Malick, D. K.; Rabuck, A. D.; Raghavachari, K.; Foresman, J. B.; Cioslowski, J.; Ortiz, J. V.; Baboul, A. G.; Stefanov, B. B.; Liu, G.; Liashenko, A.; Piskorz, P.; Komaromi, I.; Gomperts, R.; Martin, R. L.; Fox, D. J.; Keith, T.; Al-Laham, M. A.; Peng, C. Y.; Nanayakkara, A.; Gonzalez, C.; Challacombe, M.; Gill, P. M. W.; Johnson, B.; Chen, W.; Wong, M. W.; Andres, J. L.; Gonzalez, C.; Head-Gordon, M.; Replogle, E. S.; Pople, J. A. Gaussian, Inc., Pittsburgh, PA, 1998.
(28) Berger, R.; Fischer, C.; Klessinger, M. *J. Phys. Chem. A* **1998**, *102*, 7157.
(29) Doktorov, E.; Malkin, I.; Man'ko, V. *J. Mol. Spectrosc.* **1977**, *56*, 1.
(30) Dushinsky, F. *Acta Physicochim. URSS* **1937**, *7*, 551.
(31) Berger, R.; Klessinger, M. *J. Comput. Chem.* **1997**, *18*, 4887.
(32) Adler, B.; Lachowicz, A.; Thiele, K.-H. *Z. Anorg. Allg. Chem.* **1976**, *427*, 241.
(33) For another example of a rapid, unimolecular dehydrogenation of transition-metal complexes, see: Schröder, D.; Schwarz, H. *J. Am. Chem. Soc.* **1990**, *112*, 5947.

Table 1. Mass Differences (Δm)[a] Observed in the MI and CA Mass Spectra of B(1)/E(1) Mass-Selected $\mathbf{1}^+$ and Its Major Fragment Ions

		−1	−2	−15	−18	−28	−29	−30	−31	−32	−33
$\mathbf{1}^+$	MI		2					100		2	
	CA	15	1					100	15	7	6
$[\mathbf{1} - H]^+$	MI				2			100			
	CA				1			100	15	20	
$[\mathbf{1} - CH_2O]^+$	MI[b]		100		3			1			
	CA		100	5	3	1	5	10	4	1	
$[\mathbf{1} - CH_3O]^+$	MI[c]		100		1			2			
	CA		100	1				4	4	5	1
$[\mathbf{1} - \text{“}CH_4O\text{”}]^+$	MI		2		35			100			
	CA		4	5	12			100	20	2	
$[\mathbf{1} - \text{“}CH_5O\text{”}]^+$	MI		100			15		65			
	CA	1	10	1		2	3	100	2		
$[\mathbf{1} - \text{“}C_2H_5O_2\text{”}]^+$	CA[d]	15	100	20				3	10	15	
$[\mathbf{1} - \text{“}C_2H_6O_2\text{”}]^+$	CA[d]	30	40	25				100	75		
$[\mathbf{1} - \text{“}C_2H_7O_2\text{”}]^+$	CA[d]		2				3	100			

[a] Given relative to the base peak (100). For the sake of brevity, only the major signals are listed and successive fragmentations are omitted. [b] Unusually intense metastable-ion decay; the ratio between the mass-selected parent ion and the fragment due to loss of H_2 is about 18:1. [c] Unusually intense metastable-ion decay; the ratio between the mass-selected parent ion and the fragment due to loss of H_2 is about 22:1. [d] The corresponding MI spectra are very weak and most likely contaminated by CA due to residual gas present as a background in the mass spectrometer.

Scheme 2

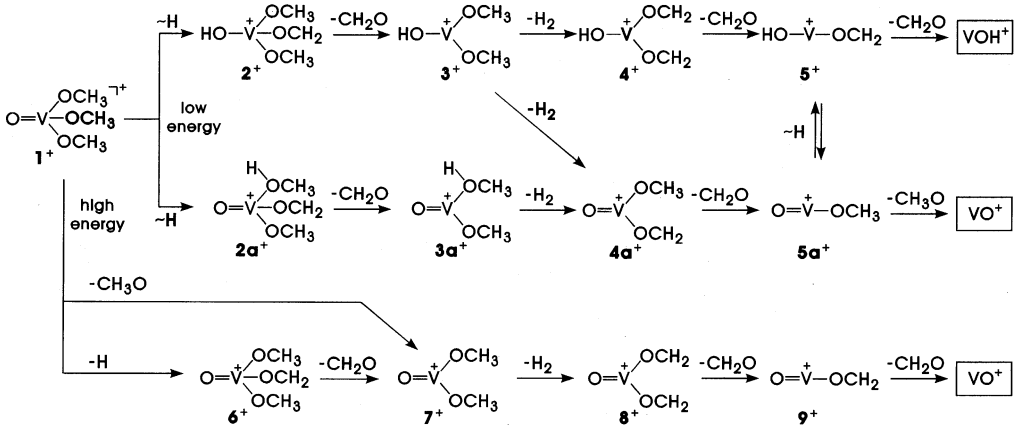

loses H_2 to yield $m/z = 128$. Likewise, loss of methoxy from $\mathbf{1}^+$ leads to $m/z = 129$ and then $m/z = 127$ via dehydrogenation.[34] The resulting product ions $[\mathbf{1} - CH_4O]^+$ and $[\mathbf{1} - CH_5O]^+$ show more diverse fragmentation patterns, although losses of formaldehyde ($\Delta m = -30$) prevail once more. Notable is the difference between the MI and CA spectra of $[\mathbf{1} - CH_5O]^+$, indicating that the losses of H_2 ($\Delta m = -2$) and CO ($\Delta m = -28$) involve low-energy pathways associated with more complex rearrangements which cannot compete with formaldehyde elimination upon CA. The next generation of daughter ions, $[\mathbf{1} - C_2H_5O_2]^+$, $[\mathbf{1} - C_2H_6O_2]^+$, and $[\mathbf{1} - C_2H_7O_2]^+$ correspond to $[VCH_nO_2]^+$ species ($n = 2-4$) and can be ascribed to losses of CO from $[\mathbf{1} - CH_5O]^+$ and expulsions of CH_2O from $[\mathbf{1} - CH_4O]^+$ and $[\mathbf{1} - CH_5O]^+$. Dehydrogenation predominates in the CA spectrum of $[\mathbf{1} - C_2H_5O_2]^+$, whereas losses of formaldehyde prevail upon CA of the two other ions. For $[\mathbf{1} - C_2H_6O_2]^+$, also a pronounced VO^+ fragment ($\Delta m = -31$) is observed, suggesting that the elimination of CH_3O is either kinetically or thermodynamically favorable for this ion. These fragmentation patterns are consistent with tentative structural assignments of these $[VCH_nO_2]^+$ ions as $OV(OCH_2)^+$ for $n = 2$, $OV(OCH_3)^+$ and/or $HOV(OCH_2)^+$ for $n = 3$, and $HOV(OCH_3)^+$ for $n = 4$.

With this information, a tentative network of the fragmentation behavior of $\mathbf{1}^+$ can be deduced (Scheme 2). Because of the obvious remaining ambiguities in terms of structural assignments, we deliberately distinguish between the experimental observables and the assigned ion structures. For example, the ionic fragment $[\mathbf{1} - CH_2O]^+$ formed upon loss of formaldehyde may correspond to either $\mathbf{3}^+$ or isomeric $\mathbf{3a}^+$. At low energies, the molecular ion $\mathbf{1}^+$ may undergo a hydrogen rearrangement ($\mathbf{1}^+ \rightarrow \mathbf{2}^+$) followed by loss of formaldehyde to afford $\mathbf{3}^+$. In this redox reaction, the formally hypervalent molecular ion $\mathbf{1}^+$ is reduced to V^{IV} in compounds $\mathbf{2}^+$ and $\mathbf{3}^+$. Alternatively, $\mathbf{1}^+$ can undergo hydrogen migration from one methoxy unit to the oxygen atom of another one, leading to the isomeric species $\mathbf{2a}^+$, from which loss of formaldehyde affords the methanol complex $\mathbf{3a}^+$. The subsequent dehydrogenation step either can proceed from $\mathbf{3}^+$ with retention of the VOH unit (formation of $\mathbf{4}^+$) or may be associated with a reconstruction of the vanadium−oxo unit in $\mathbf{4a}^+$. For $\mathbf{3a}^+$, dehydrogenation is assumed to yield $\mathbf{4a}^+$ as well. In addition, $\mathbf{4a}^+$ may be formed directly upon loss of methanol rather than CH_2O +

(34) Consecutive losses of CH_2O and H_2 have already been reported in the mass spectra of alkoxysilazanes as early as 1967; see: Silbiger J.; Lifshitz, C.; Fuchs, J.; Mandelbaum, A. *J. Am. Chem. Soc.* **1967**, *89*, 4308.

H_2 from $\mathbf{2a}^+$ (not included in Scheme 2). Assignment of structure $\mathbf{4a}^+$ to the $[\mathbf{1} - CH_4O]^+$ fragment is supported by the losses of CH_2O and CH_3O observed upon CA (Table 1). However, the expulsion of water observed in the MI spectrum of $[\mathbf{1} - CH_4O]^+$ may indicate contributions of isomeric structures (e.g., $\mathbf{4}^+$). Subsequent loss of formaldehyde from $\mathbf{4}^+$ or $\mathbf{4a}^+$ leads to $[VCH_3O_2]^+$ for which structures $\mathbf{5}^+$ and $\mathbf{5a}^+$ appear conceivable (see above). Note that $\mathbf{5}^+$ corresponds to a formal V^{II} compound, whereas conservation of the V^{IV} valence is implied in structure $\mathbf{5a}^+$. Upon collisional activation, eliminations of formaldehyde from $\mathbf{5}^+$ and of methoxy from $\mathbf{5a}^+$ lead to VOH^+ and VO^+, respectively, as the quasi-terminal fragments; the ultimate terminus is the atomic V^+ cation.[35]

The reactions of the corresponding ions resulting from initial losses of open-shell fragments are quite similar. Formation of $[\mathbf{1} - H]^+$ is assigned to α-cleavage ($\mathbf{1}^+ \rightarrow \mathbf{6}^+$), and the subsequently observed elimination of formaldehyde leads to $\mathbf{7}^+$, which is also accessible directly from $\mathbf{1}^+$ by homolytic $V-OCH_3$ bond cleavage at elevated energies. As open-shell fragments are lost from the molecular ion, structures $\mathbf{6}^+$ and $\mathbf{7}^+$ correspond to formal V^V compounds. The subsequent elimination of H_2 is assumed to be associated with a reduction to V^{III}. The assignment of structure $\mathbf{8}^+$ is supported by the almost complete absence of methoxy loss ($\Delta m = -31$) in the CA spectrum of $[\mathbf{1} - CH_5O]^+$. However, the decarbonylation observed for $[\mathbf{1} - CH_5O]^+$ points to some contribution of isomeric structures; in this respect, a formal 1,1-elimination of H_2 from $\mathbf{7}^+$ to eventually afford $HOV(OCH_3)(CO)^+$ appears reasonable.[36] Loss of formaldehyde from $\mathbf{8}^+$ is suggested to afford the formaldehyde complex $\mathbf{9}^+$, from which elimination of CH_2O leads to the VO^+ cation.

Even though these structural suggestions are consistent with the data given in Table 1, several isomeric ion structures and reaction mechanisms are conceivable. Therefore, let us consider Scheme 2 as a first assumption which shall be tested in light of the results of further experimental and theoretical studies, where we restrict ourselves to the molecular ion $\mathbf{1}^+$ and the primary fragmentations reported in this study.

3.2. Photoionization of $\mathbf{1}_D$. While the above discussion of the sector-field experiments is largely qualitative, PI studies can provide reliable absolute energetic information about ionized **1**. In view of the limited mass resolution of CERISES and the decreased sensitivity at elevated mass resolution, all PI experiments were performed with the fully deuterated compound $OV(OCD_3)_3$, $\mathbf{1}_D$.

The PI mass spectrum obtained at a photon energy of 17 eV (Figure 1a) resembles the EI mass spectrum of **1**: the molecular ion $\mathbf{1}_D^+$ and the fragment $[\mathbf{1}_D - D]^+$ are of comparable abundance, a weak signal for $[\mathbf{1}_D - D_2]^+$ is observed, and the characteristic quartet appears at $m/z = 131$, 133, 135, and 137 for the deuterated compound. In the PI studies, ions at lower masses are not considered any further

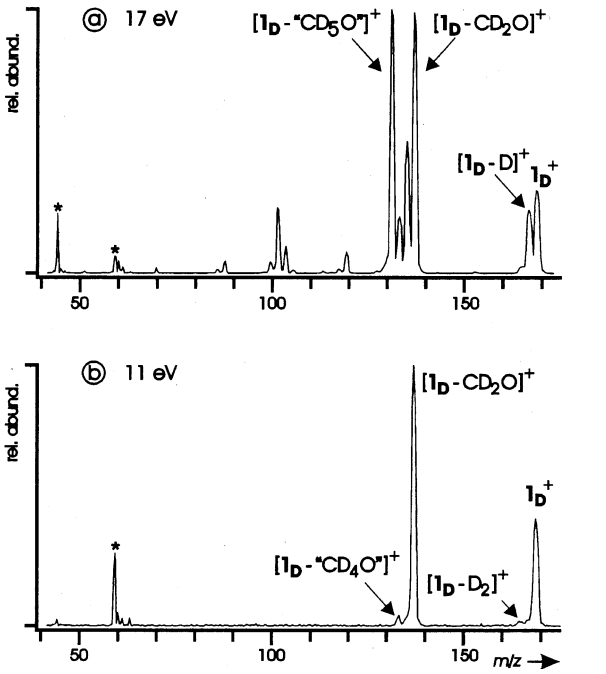

Figure 1. PI mass spectrum of $OV(OCD_3)_3$ at photon energies of (a) 17 eV and (b) 11 eV. Some of the background signals (labeled with an asterisk) are due to residual 3-methyl[4-D_1]valeramide which was present in the machine from previous experiments.

because of some interferences due to the remainder of a sample from other experiments (see the Methods). Not surprisingly, considerable changes occur at lower photon energies. The PI mass spectrum obtained with 11 eV photons (Figure 1b) is dominated by the molecular ion $\mathbf{1}_D^+$ as well as $[\mathbf{1}_D - CD_2O]^+$, whereas the other fragments are either largely suppressed or absent. Particularly, the absence of $[\mathbf{1}_D - D]^+$ and $[\mathbf{1}_D - CD_3O]^+$ ions confirms the qualitative deduction made above that the losses of open-shell fragments from $\mathbf{1}^+$ correspond to high-energy processes.

To gain quantitative information about the fragmentation routes, appearance energies (AEs) were determined by variation of the photon energy in single-ion monitoring mode. The parent ion $\mathbf{1}_D^+$ ($m/z = 169$) shows a threshold of $AE(\mathbf{1}_D^+) = 9.56 \pm 0.04$ eV (Figure 2a). The rapid rise of the ion yield above threshold is consistent with formation of the molecular ion $\mathbf{1}_D^+$ and suggests that $AE(\mathbf{1}_D^+)$ is close to the adiabatic ionization energy $IE_a(\mathbf{1}_D)$; a more detailed analysis of this aspect is presented further below. In comparison, the curves of the fragment ions rise more smoothly (Figure 2b–f)[37] in accordance with their origin in dissociative photoionization of $\mathbf{1}_D$. The lowest onset is found for loss of D_2 from the molecular ion, $AE([\mathbf{1}_D - D_2]^+) = 10.0 \pm 0.2$ eV (not shown); however, this fragment never exceeds 1% of the total photoions and is therefore not considered any further, except stating that the direct dehydrogenation of $\mathbf{1}_D^+$ appears to be subject to serious kinetic restrictions associated with a rather complex transition structure. This conclusion is further supported by the low abundance of dehydrogenation in the MI and CA spectra of $\mathbf{1}^+$ in the sector-field

(35) Schröder, D.; Engeser, M.; Schwarz, H.; Harvey, J. N. *Chem. Phys. Chem.* **2002**, *3*, 584.
(36) See also: Prüsse, T.; Fiedler, A.; Schwarz, H. *J. Am. Chem. Soc.* **1991**, *113*, 8335.
(37) From the PI threshold, the maximum yield of $\mathbf{1}^+$ is achieved in less than 0.5 eV, whereas the ions formed upon dissociative PI arise more smoothly; see Figure 2.

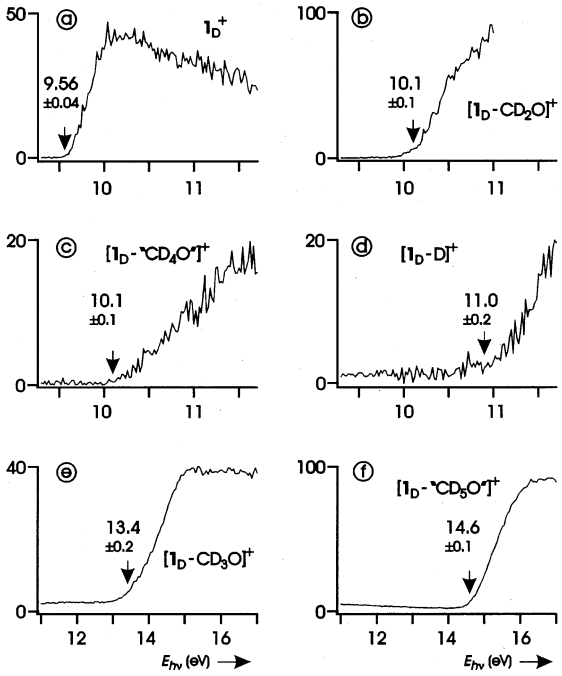

Figure 2. Single-ion monitoring of selected photoions formed from neutral $\mathbf{1}_D$ as a function of photon energy (eV) in the order of their appearance energies: (a) $\mathbf{1}_D^+$, (b) $[\mathbf{1}_D - CD_2O]^+$, (c) $[\mathbf{1}_D - CD_4O]^+$, (d) $[\mathbf{1}_D - D]^+$, (e) $[\mathbf{1}_D - CD_3O]^+$, and (f) $[\mathbf{1}_D - CD_5O]^+$. Note that the two latter spectra were recorded without a LiF window as a cutoff filter of higher-order photons. The vertical scales refer to the relative ion currents with the LiF window (a−d) and without (e, f). The corresponding appearance energies are determined by extrapolation of the linear parts of the signal onsets to the baseline (see the Methods).

experiments. With $AE([\mathbf{1}_D - CD_2O]^+) = 10.1 \pm 0.1$ eV (Figure 2b), loss of formaldehyde occurs only about 0.5 eV above the ionization threshold of neutral $\mathbf{1}_D$, suggesting that deuterium migration in $\mathbf{1}_D^+$ and subsequent loss of formaldehyde are quite facile. Within experimental uncertainty, the same threshold of $AE([\mathbf{1}_D - CD_4O]^+) = 10.1 \pm 0.1$ eV is found for the fragment assigned to the combined losses of CD_2O and D_2 (Figure 2c), even though this photofragment rises more smoothly with photon energy in comparison to $[\mathbf{1}_D - CD_2O]^+$ (Figure 2b). The finding that these two channels have more or less identical thresholds is somewhat surprising and reiterates the option that CD_3OD rather than $CD_2O + D_2$ might be formed at threshold, an issue to which we will return in more detail in the Discussion.

The energetically least demanding expulsion of a neutral open-shell fragment upon photoionization of $\mathbf{1}_D$ is loss of a D atom with $AE([\mathbf{1}_D - D]^+) = 11.0 \pm 0.2$ eV (Figure 2d). Elimination of a methoxy radical and the subsequent dehydrogenation do not occur below 11.8 eV, which is the cutoff of the LiF filter used to eliminate higher-order light emerging from the monochromator. Without the LiF filter, $AE([\mathbf{1}_D - CD_3O]^+) = 13.4 \pm 0.2$ eV and $AE([\mathbf{1}_D - CD_5O]^+) = 14.6 \pm 0.1$ eV are found for the expulsions of CD_3O and $CD_3O + D_2$, respectively (Figure 2e,f). Both values are well above the appearance energies of $\mathbf{1}_D^+$ and the ionic fragments formed upon losses of neutral closed-shell molecules. Hence, significant kinetic shifts of the threshold energies are to be expected due to competition. Nevertheless, both fragments rapidly gain in abundance once they are accessible energetically and prevail in the PI spectrum at 17 eV (Figure 1a). While pronounced competition between fragmentations to closed-shell neutrals via rearrangements and direct bond cleavages to afford open-shell neutrals is well-known in mass spectrometry, it is somewhat surprising to observe such an effect more than 3 eV above the first fragmentation thresholds. Furthermore, if one assumes an efficiently competing $V-OCD_3$ bond cleavage due to kinetic preferences of direct bond rupture, the difference of $AE([\mathbf{1}_D - CD_3O]^+) = 13.4 \pm 0.2$ eV and $AE(\mathbf{1}_D^+) = 9.56 \pm 0.04$ eV would imply in the absence of reaction barriers a dissociation energy of $D(OV(OCD_3)_2^+-OCD_3) = 3.8 \pm 0.2$ eV, which appears unrealistically large for the molecular cation of a neutral $3d^0$ compound, because ionization to the cation state must involve a bonding orbital. Inspection of the photoelectrons recorded in parallel provides a hint for an alternative explanation. Thus, the appearance of $[\mathbf{1}_D - CD_3O]^+$ at 13.4 eV coincides with the onset of a broad feature in the photoelectron spectrum of $\mathbf{1}_D$ with a maximum at about 15 eV (Figure 3).[38] This finding tentatively suggests that the loss of methoxy radical may be nascent from the ionization of the neutral compound into particular ion states which differ from the ground state of $\mathbf{1}_D^+$ in that direct $V-OCD_3$ bond cleavage is preferred (see below).

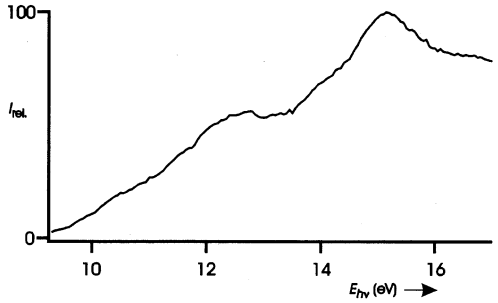

Figure 3. Photoelectron spectrum of $OV(OCD_3)_3$ in the energy window ranging from 9 to 17 eV. The photoelectron signal observed below $AE(\mathbf{1}_D) = 9.56 \pm 0.04$ eV is due to residual 3-methyl[4-D_1]valeramide from previous experiments as well as a deterioration of the electron detector in the presence of the vanadium compound.

3.3. Anionic $\mathbf{1}^-$ and a Cationized Mimic of Neutral 1. In the sector-field mass spectrometer, we also briefly investigated the behavior of the molecular anion $\mathbf{1}^-$, which can be formed upon chemical ionization (CI) of neutral **1** with N_2O as reagent gas; the actual ionizing agent is O^- formed upon dissociative electron attachment to N_2O under CI conditions. Collisional activation of $\mathbf{1}^-$ affords losses of CH_3 ($\Delta m = -15$, 100%) and CH_3O ($\Delta m = -31$, 15%) as the major fragments; two minor routes ($\Delta m = -45$ and -47, both 3%) are assigned to consecutive dissociations. The molecular anion $\mathbf{1}^-$ corresponds to a formal V^{IV} compound such that the system returns to V^V in the anionic fragment $OV(OCH_3)_2O^-$ upon the loss of the open-shell fragment CH_3.

The NR[13,14] and CR[12] mass spectra of the anion $\mathbf{1}^-$ to cationic species show rich fragmentation patterns with VO^+

(38) Note that the photoelectron spectra (PES) obtained with CERISES differ from conventional He(I) PES. In the latter, the electron energy is measured for a constant wavelength, whereas in our experiments the photon energy is varied while only electrons with kinetic energies lower than ca. 50 meV are detected.

Table 2. Relative Energies (eV) and Selected Bond Lengths (Å) and Angles (deg) of Neutral **1** and of Some Ionic Species Calculated with B3-LYP/TZVP

	$\mathbf{1}^-$	**1**	$\mathbf{1}^+$	TS $\mathbf{1}^+/\mathbf{2}^+$	$\mathbf{2}^+$	$\mathbf{3}^+$	TS $\mathbf{1}^+/\mathbf{2a}^+$	$\mathbf{2a}^+$	$\mathbf{3a}^+$	$\mathbf{4}^+$	$\mathbf{4a}^+$	$\mathbf{7}^+$
symmetry	C_s	C_{3v}	C_s	C_1	C_1	C_1[a]	C_1	C_1	C_1	C_s	C_1	C_s
E_{rel}[b]	−10.35	−9.22	0	0.83	−1.47	−0.5	0.82	−1.4	0.17	0.43[c]	0.37[d]	2.16
$r(V-{}^1O)$[e]	1.63	1.59	1.57	1.64	1.78	1.72	1.56	1.58	1.57	1.77	1.57	1.56
$r(V-{}^2O$[f]	1.87	1.77	1.88	1.91	2.00		1.90	2.03			2.01	
$r(V-{}^3O)$	1.89	1.77	1.75	1.72	1.72	1.70	1.71	1.75	1.72	1.99	1.73	1.71
$r(V-{}^4O)$[g]	1.89	1.77	1.75				1.85	2.05	2.01			
$r({}^1C-{}^2O)$	1.39	1.41	1.39	1.32	1.22		1.33	1.23			1.23	
$r({}^2C-{}^3O)$	1.39	1.41	1.42	1.43	1.42	1.43	1.45	1.47	1.43	1.23	1.43	1.44
$r(C-H)$[h]	1.10	1.09	1.09	1.32			1.28					
$r({}^1O-H)$				1.45	0.97	0.97	1.50	0.97	0.97			
$\alpha({}^1OV^2O)$	117	108	108	90	97		115	105				
$\alpha({}^1OV^3O)$	110	108	111	114	109	121	109	122	114	129	110	111
$\theta({}^1OV^2CH)$	13	0	5				−1	3	17	20	20	−6
$\theta({}^1OV^{2'}CH)$	−13	0	−5				28	33	−10	−2	−2	6

[a] Quasi-C_{2v} symmetry, since the C_{2v}-symmetrical structure is only very slightly higher in energy than the C_1-symmetrical minimum. [b] Energies (eV) relative to the cation $\mathbf{1}^+$ at 0 K. The following neutral fragments are added: CH_2O for $\mathbf{3}^+$ and $\mathbf{3a}^+$, CH_3OH for $\mathbf{4}^+$ and $\mathbf{4a}^+$, CH_3O for $\mathbf{7}^+$. [c] 1.25 eV for $\mathbf{4}^+ + CH_2O + H_2$. [d] 1.19 eV for $\mathbf{4a}^+ + CH_2O + H_2$. [e] The notation ^1O stands for the oxygen atom of the vanadyl group. [f] The notation ^2O stands for the oxygen atom of the methoxy group which isomerizes in the cation state. [g] Bond lengths to the oxygen atom which becomes part of the methanol unit in the rearrangement $\mathbf{1}^+ \rightarrow \mathbf{2a}^+$. [h] Only the bond length of the hydrogen atom which migrates in the cation state is reported. Variations in the other C−H bond lengths are less than 0.02 Å and thus not displayed.

as the base peak. For the sake of brevity, we therefore refrain from displaying the spectra as figures and list the major fragments instead (*m*/*z* ratios and abundances relative to VO^+, $m/z = 67$, in NR/CR): 159 (6/2), 130 (1/2), 129 (8/5), 128 (8/8), 127 (20/12), 113 (6/12), 99 (14/18), 98 (37/50), 97 (36/52), 84 (18/21), 83 (22/18), 68 (41/40), 67 (100/100), 51 (28/18), 31 (3/1), 30 (9/4), 29 (15/6). While neither of the two spectra bears a survivor ion ($\mathbf{1}^+$), the observed $[\mathbf{1} - H]^+$ fragment ($m/z = 159$) suggests that some species can remain almost intact. Nevertheless, quite extensive fragmentations prevail in both spectra which are assigned to occur at the cationic stage after the high-energy collision events (see below).

The difference of the NR and CR spectra is relatively small, which can be seen as an indication that the transient neutral formed upon electron detachment from $\mathbf{1}^-$ does not undergo pronounced unimolecular decompositions.[15] This conclusion is consistent with the thermal stability of neutral trialkyl vanadates(V) in the condensed phase;[39] in the particular case of neutral **1**, thermolysis was reported to afford loss of methanol.[40,41] Similar behavior is found for mass-selected $[\mathbf{1}\cdot K]^+$, a cationized mimic of neutral **1** which can be generated by electrospray ionization of a methanolic solution of **1** containing a trace of KBr.[42] Thus, the only fragments observed upon low-energy CA of $[\mathbf{1}\cdot K]^+$ at various collision energies (5−20 eV) correspond to a weak expulsion of methanol ($\Delta m = -32$) and the prevailing loss of the entire ligand **1** to afford bare K^+ as the ionic product.

4. DFT Results

The calculated structure of the neutral compound **1** belongs to the point group C_{3v} with one short V−O bond (1.59 Å) of the vanadyl unit and three equivalent, longer V−O bonds (1.77 Å) to the methoxy groups (Table 2). The methoxy units are hardly perturbed compared to either free methoxy radical or methanol. Even though the crystal structure of **1** is known, direct comparison is not sensible because solid **1** forms a bridged dimer with additional coordinations.[43] However, the two vanadyl bond lengths of 1.51 and 1.57 Å and the V−O distances to the nonbridging methoxy ligands (1.74 Å) determined in the X-ray analysis lend some confidence to our computational results.

4.1. Molecular Ions. The highest occupied molecular orbital of neutral **1** consists of nonbonding p-orbitals located at the oxygen atoms of all three methoxy groups, whereas the occupied orbitals of the vanadyl group are much lower in energy. Therefore, ionization to the molecular cation involves the methoxy manifold and is associated with a considerable lengthening of one $V-OCH_3$ bond from 1.77 Å in neutral **1** to 1.88 Å in $\mathbf{1}^+$. As a compensation, the two other $V-OCH_3$ bonds and the V−O bond of the vanadyl group are slightly shortened by 0.02 Å. These changes in geometry are reflected in the difference of the adiabatic and the vertical ionization energies of **1**. With B3-LYP/TZVP, the corresponding values are predicted as $IE_a(\mathbf{1}) = 9.25$ eV and $IE_v(\mathbf{1}) = 9.35$ eV; thus, $\Delta IE_{v/a}(\mathbf{1}) = 0.10$ eV. To evaluate the basis set dependence, further calculations with Dunning-type correlation-consistent basis sets were performed including geometry reoptimization of neutral **1**. This approach leads to a slight increase of $IE_v(\mathbf{1})$ from 9.350 eV (TZVP) to 9.381 eV (cc-pVTZ)[44] and 9.406 eV (cc-pVQZ),[45] suggesting an extrapolated value of $IE_v(\mathbf{1}) = 9.425$ eV for the complete basis-set limit.[46] Further, inclusion of zero-point energy (ZPE) lowers the adiabatic IE associated with the $0 \rightarrow 0$ transition of **1** by 0.113 eV (B3-LYP/TZVP) because the vibrational modes are somewhat weakened in the cation

(39) Lachowicz, A.; Thiele, K.-H. *Z. Anorg. Allg. Chem.* **1977**, *434*, 271.
(40) Adler, B. *Z. Anorg. Allg. Chem.* **1976**, *427*, 247.
(41) See also: Spandl, J.; Brügdam, I.; Hartl, H. *Z. Anorg. Allg. Chem.* **2000**, *626*, 2125.
(42) Further details of the electrospray experiments will be described in a forthcoming paper.
(43) Caughlan, C. N.; Smith, H. M.; Watenpaugh, K. *Inorg. Chem.* **1966**, *12*, 2131.
(44) Dunning, T. H., Jr. *J. Chem. Phys.* **1989**, *90*, 1007.
(45) Pykavy, M. Private communication, October 2002.
(46) Halkier, A.; Helgaker, T.; Jørgensen, P.; Klopper, W.; Koch, H.; Olsen, J.; Wilson, A. K. *Chem. Phys. Lett.* **1998**, *286*, 243

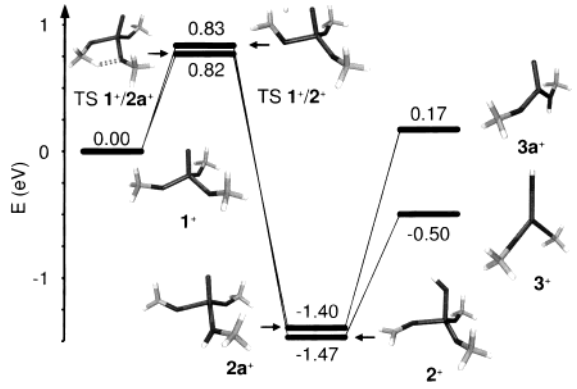

Figure 4. B3-LYP/TZVP energetics of calculated pathways from $\mathbf{1}^+$ to $\mathbf{3}^+$. The neutral fragments are omitted for the sake of clarity.

(0.100 eV for $\mathbf{1}_D$). With $\Delta IE_{v/a}(\mathbf{1}) = 0.094$ eV (B3-LYP/cc-pVQZ) and a ZPE correction of 0.113 eV (B3-LYP/TZVP), our best theoretical estimate of the ionization energy of neutral **1** at 0 K is accordingly $IE_a(\mathbf{1}) = 9.22$ eV.

Electron attachment to afford the molecular anion results in the population of low-lying d-orbitals on vanadium concomitant with formation of a V^{IV} species. Compared to neutral **1**, this also leads to a reduced symmetry of the anion $\mathbf{1}^-$, but the differences between the methoxy groups are much smaller than in the cationic case $\mathbf{1}^+$. Instead, all V−O bond distances in the anion are lengthened to a similar extent. Because these bond elongations are significant (up to 0.12 Å), the vertical electron affinity $EA_v(\mathbf{1}) = 0.31$ eV is considerably lower than the adiabatic value $EA_a(\mathbf{1}) = 1.13$ eV (1.21 eV with inclusion of ZPE). For the same reasons, the vertical electron detachment energy of the anion, $DE_v(\mathbf{1}^-) = 2.02$ eV, is significantly larger than $EA_a(\mathbf{1}) = 1.13$ eV. Finally, theory predicts that the cation $\mathbf{1}^+$ formed upon vertical removal of two electrons from $\mathbf{1}^-$ has an excess internal energy of 1.14 eV.

4.2. Primary Fragmentations. Loss of formaldehyde from the cationic species $\mathbf{1}^+$ proceeds via an initial hydrogen migration involving the methoxy group with the elongated V−O bond. The corresponding transition structure (TS) $\mathbf{1}^+/\mathbf{2}^+$ is computed to be 0.83 eV above $\mathbf{1}^+$ as schematically shown in Figure 4; also see Table 2 for further details. The optimized structure of the resulting ion is fully consistent with structure $\mathbf{2}^+$ assumed in Scheme 2: two hardly perturbed methoxy units with $r_{VO} = 1.72$ Å and $r_{CO} = 1.42$ Å are attached to the vanadium center, which bears the newly formed hydroxy ligand with $r_{VO} = 1.78$ Å and $r_{OH} = 0.97$ Å and an additional formaldehyde ligand with $r_{VO} = 2.00$ Å and $r_{CO} = 1.22$ Å. Energetically, $\mathbf{2}^+$ is 1.47 eV more stable than $\mathbf{1}^+$ such that the unimolecular rearrangement via hydrogen migration is in fact quite exothermic. Loss of the formaldehyde ligand from $\mathbf{2}^+$ barely perturbs the geometry of the remaining skeleton and requires 0.97 eV. Accordingly, not only $\mathbf{2}^+$ but also the primary fragmentation channel $\mathbf{3}^+ + CH_2O$ is lower in energy than $\mathbf{1}^+$. These considerations lead to the important conclusion that the appearance energy of the CH_2O loss determined in the photoionization experiments is subject to kinetic rather than thermodynamic control. As a consequence, the threshold can be regarded as a direct experimental measure for the barrier height associated with TS $\mathbf{1}^+/\mathbf{2}^+$. The experimental data $AE(\mathbf{1}_D^+) = 9.56 \pm 0.04$ eV and $AE(m/z = 137) = 10.1 \pm 0.1$ eV suggest a barrier of 0.54 ± 0.11 eV, which is somewhat lower than the computed value (0.83 eV at 0 K and 0.80 eV at 298 K). Note, however, that the experimental values are determined for $\mathbf{1}_D^+$ generated from the neutral sample at room temperature, such that ion dissociation may profit from the thermal energy content of the neutral compound (0.35 eV at 298 K). Therefore, some underestimation of the barrier height derived from the experimental appearance energy is expected.

Nevertheless, the difference between experiment and theory with respect to the barrier height also suggests a consideration of alternative rearrangements of $\mathbf{1}^+$. In fact, DFT predicts that a hydrogen migration from one of the methoxy groups to the oxygen atom of another CH_3O group via TS $\mathbf{1}^+/\mathbf{2a}^+$ is associated with a barrier (0.82 eV) virtually isoenergetic to TS $\mathbf{1}^+/\mathbf{2}^+$. The rearranged product $\mathbf{2a}^+$ can be described as a bisligated complex of a $OV(OCH_3)^+$ core with one methanol and one formaldehyde ligand as reflected by the elongation of two of the four V−O bonds in $\mathbf{2a}^+$ (Table 2). Energetically, $\mathbf{2a}^+$ (−1.40 eV) is slightly less stable than $\mathbf{2}^+$ (−1.47 eV). While both isomers $\mathbf{2}^+$ and $\mathbf{2a}^+$ can account for the loss of formaldehyde, the latter can also expel a methanol unit to directly afford the $[\mathbf{1} - CH_4O]^+$ fragment discussed above. Thus, theory sheds some doubt on the exclusive occurrence of the stepwise losses of $CH_2O + H_2$ in the generation of this particular fragment because the routes $\mathbf{1}^+ \rightarrow \mathbf{2}^+ \rightarrow \mathbf{3}^+ + CH_2O \rightarrow \mathbf{4}^+ + CH_2O + H_2$ and $\mathbf{1}^+ \rightarrow \mathbf{2a}^+ \rightarrow \mathbf{3a}^+ + CH_2O \rightarrow \mathbf{4a}^+ + CH_2O + H_2$ are significantly more endothermic (1.25 and 1.19 eV, respectively) than elimination of methanol, i.e., $\mathbf{1}^+ \rightarrow \mathbf{2a}^+ \rightarrow \mathbf{4a}^+ + CH_3OH$ (0.37 eV). The difference of these channels is related to the heat of hydrogenation of formaldehyde, where the computed value of 0.82 compares reasonably well, though not perfectly, with 0.95 eV derived from the literature.[7]

In the mass spectrometric experiments, also direct V−O bond cleavage concomitant with loss of a methoxy radical is observed, which presumably leads to $OV(OCH_3)_2^+$, $\mathbf{7}^+$ (Scheme 2). At 0 K, theory predicts an energy demand of 2.16 eV for the direct V−O bond cleavage $\mathbf{1}^+ \rightarrow \mathbf{7}^+ + CH_3O$. The computed structure of $\mathbf{7}^+$ is hardly perturbed compared to $\mathbf{1}^+$ with slightly shortened V−O and slightly elongated C−O bonds. Accordingly, loss of a methoxy radical should occur once the threshold energy is available. Quite remarkably, however, the computed bond energy $D(OV(OCD_3)_2^+ - OCD_3) = 2.16$ eV is significantly lower than the value of 3.8 ± 0.2 eV derived from $AE([\mathbf{1}_D - CD_3O]^+) = 13.4 \pm 0.2$ eV and $AE(\mathbf{1}_D) = 9.56 \pm 0.04$ eV in the photoionization experiments with the deuterated compound. This "delayed onset" of the CD_3O loss has already been pointed out in the context of the photoionization experiments, and we return to it further below.

5. Discussion

The combination of different mass spectrometric methods with theoretical studies provides quite detailed insight into the fragmentation behavior of ionized **1** and the associated

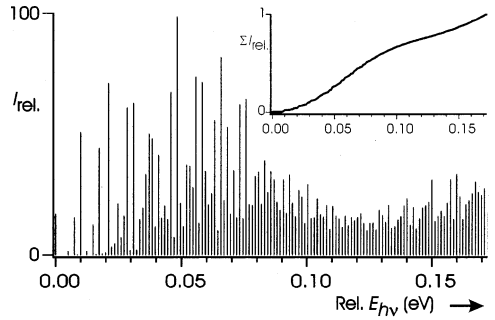

Figure 5. Low energy part of the calculated Franck−Condon envelope for the ionization of neutral $OV(OCD_3)_3$ from its vibronic ground state to the monocation in its lowest electronic doublet state. The abscissa shows the photon energy (eV) in excess of the 0 → 0 transition energy. Each of the vertical lines in the spectrum represents the sum of the Franck−Condon factors belonging to transitions within a given energy interval (constant width of 1.24 meV) with the most intense peak being normalized to 100. The inset displays the resulting sum profile.

energetics. Yet, several problems remain, which are addressed here as far as the molecular ions and the primary fragments are concerned.

5.1. Photoionization. Above, we indirectly implied that photoionization of neutral **1** can proceed more or less adiabatically; hence, $IE_a(\mathbf{1}) \approx AE(\mathbf{1}_D^+) = 9.56 \pm 0.04$ eV. However, the theoretical study reveals a change in symmetry between the neutral and cationic species **1** and $\mathbf{1}^+$. To address this aspect more quantitatively, the Franck−Condon envelope for the transition $\mathbf{1}_D \rightarrow \mathbf{1}_D^+$ has been calculated. Note, however, that the Franck−Condon profile has been computed within the harmonic approximation and has therefore to be viewed with some caution. In particular, for $\mathbf{1}_D^+$ the interconversion between various symmetry-equivalent structures is feasible at lower internal energies, which is not taken into account in the harmonic approach. Inspection of Figure 5 shows that the 0 → 0 transition has a nonnegligible intensity, but other transitions are much more favorable.

The computed Franck−Condon profile can be used to refine the evaluation of $IE_a(\mathbf{1})$ from the experimental data. To this end, the onset of the photoion yield of $\mathbf{1}_D^+$ (Figure 2a) is overlaid with a summation of the calculated Franck−Condon envelope for the transition $\mathbf{1}_D \rightarrow \mathbf{1}_D^+$. With this approach, $IE_a(\mathbf{1}_D) = 9.55 \pm 0.05$ eV is derived, which converts to a final value of $IE_a(\mathbf{1}) = 9.54 \pm 0.05$ eV for the unlabeled compound after inclusion of the calculated differences in ZPE. This experimental value is in reasonable, though not perfect, agreement with the theoretical estimate of $IE_a(\mathbf{1}) = 9.22$ eV derived above.

5.2. Losses of Odd-Electron versus Even-Electron Neutrals. The photoionization experiments reveal a surprisingly large appearance energy for the elimination of the open-shell fragment CD_3O from the molecular ion $\mathbf{1}^+$. Formally, this process would correspond to a homolytic V−O bond cleavage for which the difference between the AE of about 13.4 eV and $IE_a(\mathbf{1}) = 9.54 \pm 0.05$ eV imply an energy demand of almost 4 eV. Instead, the DFT calculations suggest $D(OV(OCH_3)_2^+-OCH_3) = 2.16$ eV. Some delay in the threshold for the formation of $\mathbf{7}^+$ might be attributed to a kinetic shift[47] arising from the competing unimolecular rearrangement in the course of CH_2O loss from $\mathbf{1}^+$ (see above). Nevertheless, the observed difference is unexpectedly large. Moreover, once the photofragmentation threshold is reached, the elimination of methoxy rapidly gains in abundance, thereby contradicting the assumption of a pronounced kinetic shift of this channel due to mere competition. As mentioned above, photoionization to excited cation states may provide an alternative explanation for the experimentally observed behavior. Thus, the AE of the CD_3O loss coincides with the onset of an additional feature in the photoelectron spectrum of $\mathbf{1}_D$. This observation suggests that at about 4 eV above the photoionization threshold some ion states can be formed for which direct V−OCD_3 bond rupture is preferred. This aspect can be evaluated more accurately by means of time-dependent DFT calculations of the electronically excited states of the cation. In addition to the ground-state configuration, these calculations reveal eight excited cation states within 3.2 eV relative to $\mathbf{1}^+$, while a much larger number of states emerge above 3.7 eV (e.g., 24 excited states lying between 4 and 5 eV relative to $\mathbf{1}^+$). Accordingly, we propose that, at photon energies below 13.4 eV, photoionization leads to $\mathbf{1}^+$ and its primary photofragments involving losses of neutral closed-shell molecules. Even though theory suggests that the loss of methoxy could already occur at photon energies above 11.7 eV, competition and energy carried away by the leaving photoelectron suppress this channel. Instead, the manifold of excited cation states arising ca. 4 eV above $\mathbf{1}^+$ may allow for a quasi-resonant adsorption of photons and thereby the formation of highly excited cations which rapidly dissociate. For these ions with high internal energy content, direct bond rupture leading to methoxy loss is likely to be entropically preferred compared to the more complex hydrogen rearrangements involved in the formation of the neutral closed-shell fragments discussed above. While a solid foundation of this argument would require a dynamical treatment of the excited cation states, on the basis of the experimental and theoretical information available we consider this picture as a quite reasonable explanation for the "delayed" but then steep onset for the loss of CD_3O (and $CD_3O + D_2$) upon photoionization of $\mathbf{1}_D$.

5.3. $CH_2O + H_2$ versus CH_3OH Loss. One specific divergence between the various experimental and theoretical results has been addressed several times so far, while not being treated explicitly. Thus, the B3-LYP calculations predict that the formation of $\mathbf{3}^+ + CH_2O$ is exothermic and that of $\mathbf{3a}^+ + CH_2O$ only slightly endothermic relative to $\mathbf{1}^+$, whereas the subsequent dehydrogenations to either $\mathbf{4}^+$ or $\mathbf{4a}^+$ are considerably endothermic (between 1.25 and 1.19 eV, respectively, for $CH_2O + H_2$ as the neutral products). In contrast, the photoionization thresholds of $[\mathbf{1}_D - CD_2O]^+$ and $[\mathbf{1}_D - CD_4O]^+$ coincide within experimental error.

As outlined above, the formations of either $\mathbf{3}^+$ or $\mathbf{3a}^+$ are subject to kinetic control. The barrier heights computed for the dissociations of energized $\mathbf{1}^+$ via $\mathbf{2}^+$ to $\mathbf{3}^+ + CH_2O$ and via $\mathbf{2a}^+$ to $\mathbf{3a}^+ + CH_2O$ therefore indicate that the fragments $\mathbf{3}^+$ and $\mathbf{3a}^+$ may contain considerable excess internal energy.

(47) Lifshitz, C. *Eur. J. Mass Spectrom.* **2002**, *8*, 85 and references therein.

Combination of the photoionization threshold $AE([\mathbf{1}_D - CD_2O]^+) = 10.1 \pm 0.1$ eV and $IE_a(\mathbf{1}) = 9.54 \pm 0.05$ eV with the calculated energetics of $\mathbf{1}^+$, $\mathbf{3}^+$, and $\mathbf{3a}^+$ suggests excess internal energies of about 1.1 eV for $\mathbf{3}^+$ and 0.4 eV for $\mathbf{3a}^+$. Nevertheless, even these amounts of internal energy cannot explain the identical appearance energies of the fragments $[\mathbf{1}_D - CD_2O]^+$ and $[\mathbf{1}_D - CD_4O]^+$. An alternative explanation of the experimental findings is that at threshold energies not only loss of formaldehyde from $\mathbf{1}^+$ can occur (either $\mathbf{1}^+ \rightarrow \mathbf{2}^+ \rightarrow \mathbf{3}^+$ or $\mathbf{1}^+ \rightarrow \mathbf{2a}^+ \rightarrow \mathbf{3a}^+$), but hydrogen migration can also lead to the formation of a methanol unit which is then expelled as an intact neutral molecule ($\mathbf{1}^+ \rightarrow \mathbf{2a}^+ \rightarrow \mathbf{4a}^+$). In fact, the difference of $\Delta_f H(CH_3OH)$ and $\sum\Delta_f H(CH_2O + H_2)$ of 0.95 eV fills the gap between the calculated energy demand for the combined losses of $CH_2O + H_2$ and the experimentally observed threshold for dissociative photoionization to $[\mathbf{1}_D - CD_4O]^+$. Accordingly, we propose that loss of methanol is preferred close to the fragmentation threshold, whereas the sequential route of first losing formaldehyde and then dihydrogen can only compete at elevated energies.

5.4. Reaction Mechanism. Quite interestingly, the theoretical studies indicate that the initially occurring hydrogen migration of ionized $\mathbf{1}^+$ can proceed via two independent routes, which are more or less isoenergetic. In both cases, hydrogen migration commences from the methoxy group in $\mathbf{1}^+$ which bears an elongated V−O bond after ionization and then proceeds either to the vanadyl unit ($\mathbf{1}^+ \rightarrow \mathbf{2}^+$) or to the oxygen atom of another methoxy group ($\mathbf{1}^+ \rightarrow \mathbf{2a}^+$). The former reaction involves oxidation of one methoxy unit to formaldehyde in analogy to oxidation reactions mediated by high-valent transition-metal oxides.[1,2] The latter proceeds as a disproportionation of two methoxy units in analogy to the reactions of metal ions with dimethyl peroxide.[48] Apparently, both mechanisms can effectively compete in the particular case of $\mathbf{1}^+$, indicating the ambivalent behavior of this compound. On one hand, the vanadium center bears a tendency for oxidation reactions, while conservation of the vanadyl unit is favorable on the other hand. Even though the experimental data do not allow a distinction between both mechanisms, the apparent loss of methanol directly from the molecular ion $\mathbf{1}^+$ may serve as an indication for the participation of TS $\mathbf{1}^+/\mathbf{2a}^+$.

5.5. Vertical Electron Transfer. Finally, let us briefly return to the extensive fragmentation observed in the NR and CR spectra of the molecular anion $\mathbf{1}^-$. After having understood the energetics for the dissociation of $\mathbf{1}^+$, we attribute the fragmentations upon NR and CR to the energy deposition upon vertical electron transfer occurring in the collisions. Thus, theory predicts that vertical detachment of two electrons from $\mathbf{1}^-$ results in a cationic species having about 1.14 eV excess internal energy; in addition, a considerable amount of energy may be deposited in the kiloelectronvolt collisions. Because the photoionization experiments reveal that the threshold for loss of formaldehyde from $\mathbf{1}^+$ is only on the order of 0.5 eV, the excessive fragmentation behavior can therefore be attributed to the facile dissociation of the cationic species, whereas the molecular anion $\mathbf{1}^-$ and neutral **1** appear to be quite stable.

(48) Schalley, C. A.; Wesendrup, R.; Schröder, D.; Weiske, T.; Schwarz, H. *J. Am. Chem. Soc.* **1995**, *117*, 7711.

6. Conclusions

Combined experimental and theoretical approaches elucidate the energetics and mechanisms of the primary fragmentation of the molecular cation of trimethyl vanadate(V), $\mathbf{1}^+$, to a considerable extent. A particular hallmark is the quite important experimental information about the barrier height for loss of CH_2O from the cation $\mathbf{1}^+$, which provides a direct observable for a unimolecular rearrangement in a prototype V/O system. The present results may therefore be used to evaluate the performance of various theoretical approaches for the description of barrier heights in vanadium oxide catalysis. In this respect, our DFT calculations appear to somewhat overestimate the reaction barrier for the rearrangement of the methoxy substituents in $\mathbf{1}^+$. Surprisingly, however, the theoretical results also indicate that at the very threshold two kinds of more or less isoenergetic rearrangements of $\mathbf{1}^+$ can compete with each other: (i) hydrogen transfer from one methoxy group to the vanadyl unit via TS $\mathbf{1}^+/\mathbf{2}^+$ and (ii) hydrogen transfer from one methoxy group to the O atom of another one via TS $\mathbf{1}^+/\mathbf{2a}^+$. On the basis of the present experimental data, we cannot decide which of the two TSs is more relevant, but most likely both of them play a role in the dissociation of $\mathbf{1}^+$.

As far as the consecutive fragmentations are concerned, the sector-field experiments only provide limited insight because the number of conceivable structural isomers is too large, while the fragmentations observed may be determined by thermochemical preferences or kinetic criteria including possible restrictions imposed by spin multiplicity. Accordingly, a more concise analysis of these secondary fragments requires both complementary experimental studies and additional theoretical work which will be addressed in a forthcoming paper.

Acknowledgment. Continuous financial support by the Sonderforschungsbereich 546, the Deutsche Forschungsgemeinschaft, the Fonds der Chemischen Industrie, the Volkswagen-Stiftung, and the Gesellschaft von Freunden der Technischen Universität Berlin is gratefully acknowledged. Further, we thank the Konrad-Zuse Institut for the allocation of computer time and the staff of LURE for operating the Super-ACO ring and the adjacent facilities.

IC030264X